ARTICLE

doi:10.1038/nature09760

A closely packed system of low-mass, low-density planets transiting Kepler-11

Jack J. Lissauer[1], Daniel C. Fabrycky[2], Eric B. Ford[3], William J. Borucki[1], Francois Fressin[4], Geoffrey W. Marcy[5], Jerome A. Orosz[6], Jason F. Rowe[7], Guillermo Torres[4], William F. Welsh[6], Natalie M. Batalha[8], Stephen T. Bryson[1], Lars A. Buchhave[9], Douglas A. Caldwell[7], Joshua A. Carter[4], David Charbonneau[4], Jessie L. Christiansen[7], William D. Cochran[10], Jean-Michel Desert[4], Edward W. Dunham[11], Michael N. Fanelli[12], Jonathan J. Fortney[2], Thomas N. Gautier III[13], John C. Geary[4], Ronald L. Gilliland[14], Michael R. Haas[1], Jennifer R. Hall[15], Matthew J. Holman[4], David G. Koch[1], David W. Latham[4], Eric Lopez[2], Sean McCauliff[15], Neil Miller[2], Robert C. Morehead[3], Elisa V. Quintana[7], Darin Ragozzine[4], Dimitar Sasselov[4], Donald R. Short[6] & Jason H. Steffen[16]

When an extrasolar planet passes in front of (transits) its star, its radius can be measured from the decrease in starlight and its orbital period from the time between transits. Multiple planets transiting the same star reveal much more: period ratios determine stability and dynamics, mutual gravitational interactions reflect planet masses and orbital shapes, and the fraction of transiting planets observed as multiples has implications for the planarity of planetary systems. But few stars have more than one known transiting planet, and none has more than three. Here we report Kepler spacecraft observations of a single Sun-like star, which we call Kepler-11, that reveal six transiting planets, five with orbital periods between 10 and 47 days and a sixth planet with a longer period. The five inner planets are among the smallest for which mass and size have both been measured, and these measurements imply substantial envelopes of light gases. The degree of coplanarity and proximity of the planetary orbits imply energy dissipation near the end of planet formation.

Kepler is a 0.95-m-aperture space telescope using transit photometry to determine the frequency and characteristics of planets and planetary systems[1–4]. The only fully validated multiple transiting planet system to appear in the literature to date is Kepler-9, with two giant planets[5] orbiting exterior to a planet whose radius is only 1.6 times that of Earth[6]. The Kepler-10 system[7] contains one confirmed planet and an additional unconfirmed planetary candidate. Light curves of five other Kepler target stars, each with two or three (unverified) candidate transiting planets, have also been published[8]. A catalogue of all candidate planets, including targets with multiple candidates, is presented in ref. 35.

We describe below a six-planet system orbiting a star that we name Kepler-11. First, we discuss the spacecraft photometry on which the discovery is based. Second, we summarize the stellar properties, primarily constrained using ground-based spectroscopy. Then we show that slight deviations of transit times from exact periodicity owing to mutual gravitational interactions confirm the planetary nature of the five inner candidates and provide mass estimates. Next, the outer planet candidate is validated by computing an upper bound on the probability that it could result from known classes of astrophysical false positives. We then assess the dynamical properties of the system, including long-term stability, eccentricities and relative inclinations of the planets' orbital planes. We conclude with a discussion of constraints on the compositions of the planets and the clues that the compositions of these planets and their orbital dynamics provide for the structure and formation of planetary systems.

Kepler photometry

The light curve of the target star Kepler-11 is shown in Fig. 1. After detrending, six sets of periodic dips of depth of roughly one millimagnitude (0.1%) can be seen. When the curves are phased with these six periods, each set of dips (Fig. 2) is consistent with a model[9] of a dark, circular disk masking out light from the same limb-darkened stellar disk; that is, evidence of multiple planets transiting the same star. We denote the planets in order of increasing distance from the star as Kepler-11b, Kepler-11c, Kepler-11d, Kepler-11e, Kepler-11f and Kepler-11g.

Background eclipsing binary stars can mimic the signal of a transiting planet[10]. Kepler returns data for each target as an array of pixels, enabling post-processing on the ground to determine the shift, if any, of the location of the target during the apparent transits. For all six planetary candidates of Kepler-11, these locations are coincident, with 3σ uncertainties of 0.7 arcseconds or less for the four largest planets and 1.4 arcseconds for the two smallest planets; see the first section of the Supplementary Information and Supplementary Table 1 for details. This lack of displacement during transit substantially restricts the parameter space available for background eclipsing binary star false positives.

Supplementary Table 2 lists the measured transit depths and durations for each of the planets. The durations of the drops in flux caused by three of the planets are consistent with near-central transits of the same star by planets on circular orbits. Kepler-11e's transits are one-third shorter than expected, implying an inclination to the plane of the sky of 88.8° (orbital eccentricity can also affect transit duration, but

[1]NASA Ames Research Center, Moffett Field, California 94035, USA. [2]UCO/Lick Observatory, University of California, Santa Cruz, California 95064, USA. [3]University of Florida, 211 Bryant Space Science Center, Gainesville, Florida 32611-2055, USA. [4]Harvard-Smithsonian Center for Astrophysics, 60 Garden Street, Cambridge, Massachusetts 02138, USA. [5]Department of Astronomy, UC Berkeley, Berkeley, California 94720, USA. [6]San Diego State University, 5500 Campanile Drive, San Diego, California 92182, USA. [7]SETI Institute/NASA Ames Research Center, Moffett Field, California 94035, USA. [8]Department of Physics and Astronomy, San Jose State University, One Washington Square, San Jose, California 95192, USA. [9]Niels Bohr Institute, Copenhagen University, Juliane Maries Vej 30, DK-2100 Copenhagen, Denmark. [10]McDonald Observatory, The University of Texas at Austin, Austin, Texas 78712-0259, USA. [11]Lowell Observatory, 1400 W. Mars Hill Road, Flagstaff, Arizona 86001, USA. [12]Bay Area Environmental Research Inst./NASA Ames Research Center, Moffett Field, California 94035, USA. [13]Jet Propulsion Laboratory, 4800 Oak Grove Drive, Pasadena, California 91109, USA. [14]Space Telescope Science Institute, 3700 San Martin Drive, Baltimore, Maryland 21218, USA. [15]Orbital Sciences Corporation/NASA Ames Research Center, Moffett Field, California 94035, USA. [16]Fermilab Center for Particle Astrophysics, MS 127, PO Box 500, Batavia, Illinois 60510, USA.

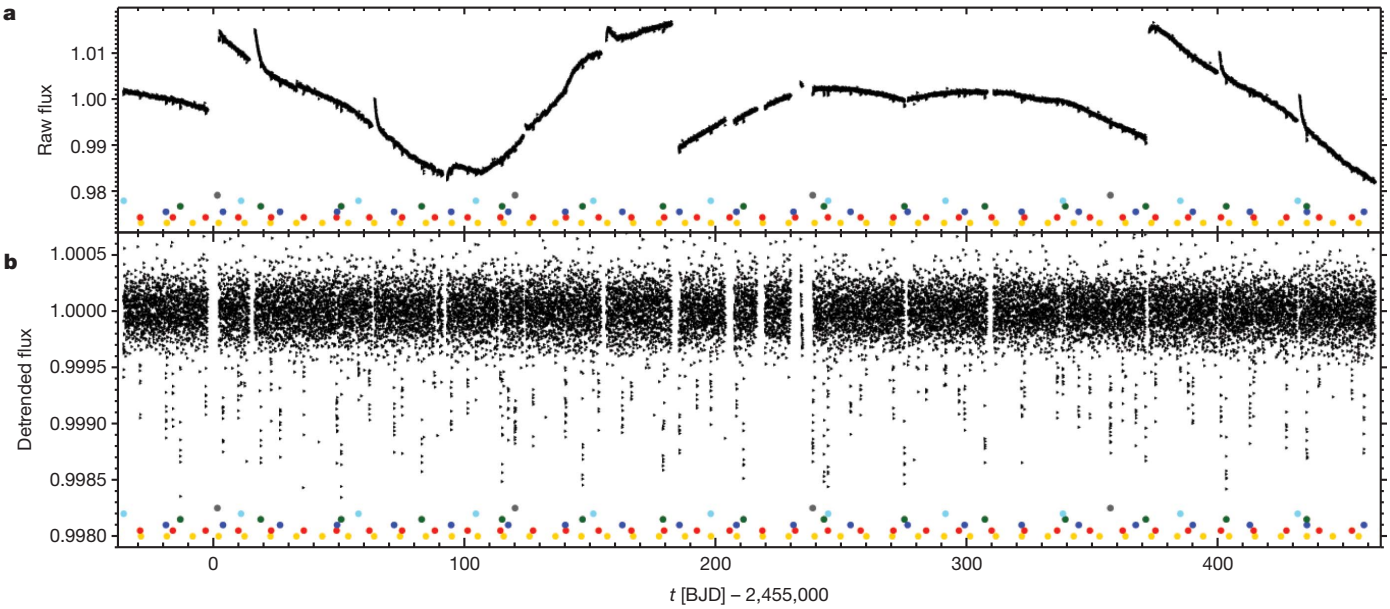

Figure 1 | Light curves of Kepler-11, raw and detrended. Kepler-11 is a G dwarf star with Kepler magnitude of 13.7, visual magnitude of 14.2 magnitudes, and celestial coordinates RA = 19 h 48 min 27.62 s, dec. = +41° 54′ 32.9″; alternative designations used in catalogues are KIC 6541920 and KOI-157. Kepler-11 is about 2,000 light-years from Earth. Variations in the brightness of Kepler-11 have been monitored with an effective duty cycle of 91% over the time interval barycentric Julian date (BJD) 2,454,964.511 to 2,455,462.296, with data returned to Earth at a long cadence of 29.426 min. Shown are Kepler photometric data, raw from the spacecraft with each quarter normalized to its median (**a**) and after detrending with a polynomial filter (**b**)[31]; *t* represents time in days since BJD 2,455,000. These data are available from the MAST archive at http://archive.stsci.edu/kepler/. Note the difference in vertical scales between the two panels. The six sets of periodic transits are indicated with dots of differing colours. Four photometric data points representing the triply concurrent transit of planets Kepler-11b, Kepler-11d and Kepler-11e at BJD 2,455,435.2 (Supplementary Fig. 12) are not shown because their values lie below the plotted range. Data have also been returned for this target star at a cadence of 58.85 s since BJD 2,455,093.215, but our analysis is based exclusively on the long cadence data.

the eccentricity needed to explain this duration for a central transit would destabilize the system). The transit durations of planets Kepler-11b and Kepler-11f suggest somewhat non-central transits. In sum, the light curve shapes imply that the system is not perfectly coplanar: Kepler-11g and Kepler-11e are mutually inclined by at least ~0.6°.

Ground-based spectroscopy

We performed a standard spectroscopic analysis[11,12] of a high-resolution spectrum of Kepler-11 taken at the Keck I telescope. We derive an effective temperature of $T_{\rm eff} = 5{,}680 \pm 100$ K, surface gravity g of $\log[g\ ({\rm cm\,s^{-2}})] = 4.3 \pm 0.2$, metallicity of $[{\rm Fe/H}] = 0.0 \pm 0.1$ dex, and an projected stellar equatorial rotation of $v\sin i = 0.4 \pm 0.5\ {\rm km\,s^{-1}}$. Combining these measurements with stellar evolutionary tracks[13,14] yields estimates of the star's mass, $0.95 \pm 0.10\ M_{\odot}$, and radius, $1.1 \pm 0.1\ R_{\odot}$, where the subscript $\odot$ signifies solar values. Estimates of the stellar density based upon transit observations are consistent with these spectroscopically determined parameters. Therefore, we adopt these stellar values for the rest of the paper, and note that the planet radii scale linearly with the stellar radius. Additional details on these studies are provided in section 2 of the Supplementary Information.

Transit timing variations

Transits of a single planet on a Keplerian orbit about its star must be strictly periodic. In contrast, the gravitational interactions among planets in a multiple planet system cause planets to speed up and slow down by small amounts, leading to deviations from exact periodicity of transits[15,16]. Such variations are strongest when planetary orbital periods are commensurate or nearly so, which is the case for the giant planets Kepler-9b and Kepler-9c (ref. 5), or when planets orbit close to one another, which is the case for the inner five transiting planets of Kepler-11.

The transit times of all six planets are listed in Supplementary Table 2. Deviations of these times from the best-fitting linear ephemeris (transit timing variations, or TTVs) are plotted in Fig. 3. We modelled these deviations with a system of coplanar, gravitationally interacting planets using numerical integrations[5,17] (Supplementary Information). The TTVs for each planet are dominated by the perturbations from its immediate neighbours (Supplementary Fig. 5). The relative periods and phases of each pair of planets, and to a lesser extent the small eccentricities, determine the shapes of the curves in Fig. 3; the mass of each perturber determines the amplitudes. Thus this TTV analysis allows us to estimate the masses of the inner five planets and to place constraints on their eccentricities. We report the main results in Table 1 and detailed fitting statistics in Supplementary Fig. 5 and associated text).

Perturbations of planets Kepler-11d and Kepler-11f by planet Kepler-11e are clearly observed. These variations confirm that all three sets of transits are produced by planets orbiting the same star and yield a 4σ detection of the mass of Kepler-11e. Somewhat weaker perturbations are observed in the opposite direction, yielding a 3σ detection of the mass of Kepler-11d and a 2σ detection of the mass of Kepler-11f.

The inner pair of observed planets, Kepler-11b and Kepler-11c, lie near a 5:4 orbital period resonance and strongly interact with one another. The degree to which they deviate from exact resonance determines the frequency at which their TTVs should occur. Even though the precision of individual transit times is low owing to small transit depths, transit-timing periodograms of both planets show peak power at the expected frequency (Supplementary Fig. 4). The TTVs thus confirm that Kepler-11b and Kepler-11c are planets, confirm that they orbit the same star, and yield 2σ determinations of their masses. The outer planet, Kepler-11g, does not strongly interact with the others; it would need to be unexpectedly massive ($\sim 1\ M_{\rm Jupiter}$) to induce a detectable ($\Delta\chi^2 = 9$) signal on the entire set of transit mid-times.

Validation of planet Kepler-11g

The outer planetary candidate is well-separated from the inner five in orbital period, and its dynamical interactions are not manifested in the

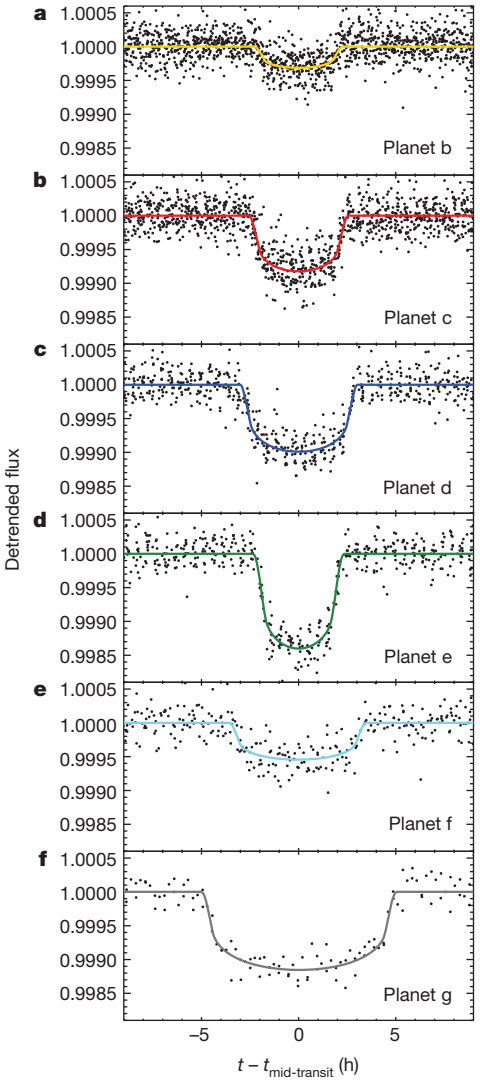

Figure 2 | Detrended data of Fig. 1 shown phased at the period of each transit signal and zoomed to an 18-h region around mid-transit. Overlapping transits are not shown, nor were they used in the model. Each panel has an identical vertical scale, to show the relative depths, and identical horizontal scale, to show the relative durations. The colour of each planet's model light curve matches the colour of the dots marking its transits in Fig. 1.

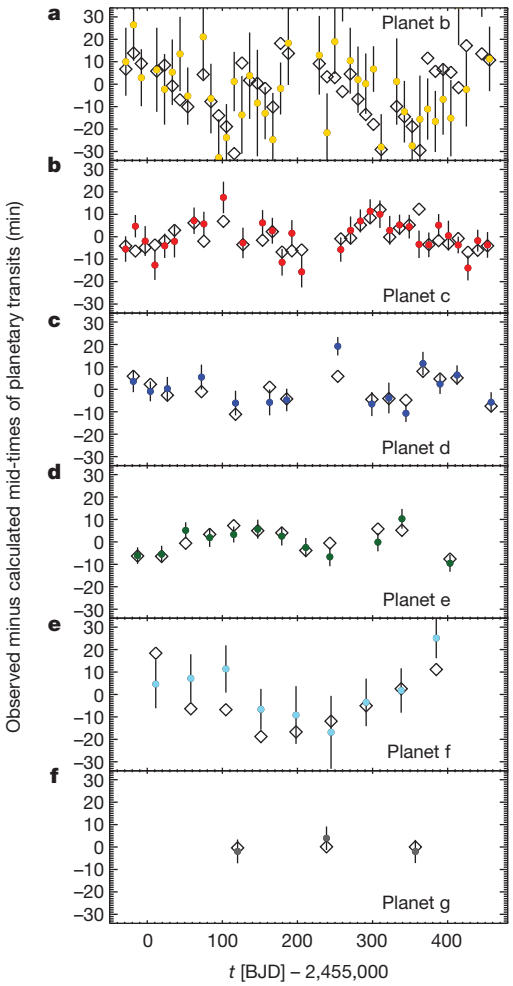

Figure 3 | Transit timing variations and dynamical fits. Observed mid-times of planetary transits (see section 3 of the Supplementary Information for transit-fitting method and Supplementary Table 2 for transit times) minus a calculated linear ephemeris, are plotted as dots with 1σ error bars; colours correspond to the planetary transit signals in Figs 1 and 2. The times derived from the 'circular fit' model described in Supplementary Table 4 are given by the open diamonds. Contributions of individual planets to these variations are shown in Supplementary Fig. 6a.

data presently available. Thus, we only have a weak upper bound on its mass, and unlike the other five candidates, its planetary nature is not confirmed by dynamics. The signal (Fig. 2f) has the characteristics of a transiting planet and is far too large to have a non-negligible chance of being due to noise, but the possibility that it could be an astrophysical false-positive must be addressed. To obtain a Bayesian estimate of the probability that the events seen are due to a sixth planet transiting the star Kepler-11, we must compare estimates of the a priori likelihood of such a planet and of a false positive. This is the same basic methodology as was used to validate planet Kepler-9d (ref. 6).

We begin by using the BLENDER code[6] to explore the wide range of false positives that might mimic the Kepler-11g signal, by modelling the light curve directly in terms of a blend scenario. The overwhelming majority of such configurations are excluded by BLENDER. We then use all other observational constraints to rule out additional blends, and we assess the a priori likelihood of the remaining false positives. Two classes of false positives were considered: (1) the probability of an eclipsing pair of objects that is physically associated with Kepler-11 providing as good a fit to the Kepler data as provided by a planet transiting the primary star was found to be 0.31×10^{-6}; (2) the probability that a background eclipsing binary or star + planet pair yielding a signal of appropriate period, depth and shape could be present and not have been detected as a result of a centroid shift in the in-transit data, or other constraints from spectroscopy and photometry, was found to be 0.58×10^{-6}. Thus the total a priori probability of a signal mimicking a planetary transit is 0.89×10^{-6}. There is a 0.5×10^{-3} a priori probability of a transiting sixth planet in the mass–period domain. This value was conservatively estimated (not accounting for the coplanarity of the system; the value would increase by an order of magnitude if we were to assume an inclination distribution consistent with seeing transits of the five inner planets) using the observed distribution of extrasolar planets[18,19]. Details of these calculations are presented in section 5 of the Supplementary Information and Supplementary Figs 8–11. Taking the ratio of these probabilities yields a total false alarm probability of 1.8×10^{-3}, which is small enough for us to consider Kepler-11g to be a validated planet.

Long-term stability and coplanarity

One of the most striking features about the Kepler-11 system is how close the orbits of the planets are to one another. From suites of numerical integrations[20], dynamical survival of systems with more than three comparably spaced planets for at least 10^{10} orbits has been shown only if the spacing between orbital semi-major axes ($a_o - a_i$) exceeds a critical

Table 1 | Planet properties

Planet	Period (days)	Epoch (BJD)	Semi-major axis (AU)	Inclination (°)	Transit duration (h)	Transit depth (millimagnitude)	Radius ($R_\oplus$)	Mass ($M_\oplus$)	Density (g cm^{-3})
b	10.30375 ± 0.00016	2,454,971.5052 ± 0.0077	0.091 ± 0.003	$88.5^{+1.0}_{-0.6}$	4.02 ± 0.08	0.31 ± 0.01	1.97 ± 0.19	$4.3^{+2.2}_{-2.0}$	$3.1^{+2.1}_{-1.5}$
c	13.02502 ± 0.00008	2,454,971.1748 ± 0.0031	0.106 ± 0.004	$89.0^{+1.0}_{-0.6}$	4.62 ± 0.04	0.82 ± 0.01	3.15 ± 0.30	$13.5^{+4.8}_{-6.1}$	$2.3^{+1.3}_{-1.1}$
d	22.68719 ± 0.00021	2,454,981.4550 ± 0.0044	0.159 ± 0.005	$89.3^{+0.6}_{-0.4}$	5.58 ± 0.06	0.80 ± 0.02	3.43 ± 0.32	$6.1^{+3.1}_{-1.7}$	$0.9^{+0.5}_{-0.3}$
e	31.99590 ± 0.00028	2,454,987.1590 ± 0.0037	0.194 ± 0.007	$88.8^{+0.2}_{-0.2}$	4.33 ± 0.07	1.40 ± 0.02	4.52 ± 0.43	$8.4^{+2.5}_{-1.9}$	$0.5^{+0.2}_{-0.2}$
f	46.68876 ± 0.00074	2,454,964.6487 ± 0.0059	0.250 ± 0.009	$89.4^{+0.3}_{-0.2}$	6.54 ± 0.14	0.55 ± 0.02	2.61 ± 0.25	$2.3^{+2.2}_{-1.2}$	$0.7^{+0.7}_{-0.4}$
g	118.37774 ± 0.00112	2,455,120.2901 ± 0.0022	0.462 ± 0.016	$89.8^{+0.2}_{-0.2}$	9.60 ± 0.13	1.15 ± 0.03	3.66 ± 0.35	<300	–

$R_\oplus$, radius of the Earth; $M_\oplus$, mass of the Earth. Planetary periods and transit epochs are the best-fitting linear ephemerides. Periods are given as viewed from the barycentre of our Solar System. Because Kepler-11 is moving towards the Sun with a radial velocity of 57 km s^{-1} (Supplementary Fig. 1), actual orbital periods in the rest frame of Kepler-11 are a factor of 1.00019 times as long as the values quoted. Uncertainty in epoch is median absolute deviation of transit times from this ephemeris; uncertainty in period is this quantity divided by the number of orbits between the first and last observed transits. Radii are from Supplementary Table 2; uncertainties represent 1σ ranges, and are dominated by uncertainties in the radius of the star. The mass estimates are the uncertainty-weighted means of the three dynamical fits (Supplementary Table 4) to TTV observations (Supplementary Table 2) and the quoted ranges cover the union of 1σ ranges of these three fits. One of these fits constrains all of the planets to be on circular orbits, the second one allows only planets Kepler-11b and Kepler-11c to have eccentric orbits, and the third solves for the eccentricities of all five planets Kepler-11b to Kepler-11f; see section 4 of the Supplementary Information. Stability considerations may preclude masses near the upper ends of the quoted ranges for the closely spaced inner pair of planets. Inclinations are with respect to the plane of the sky.

number ($\Delta_{\rm crit} \gtrsim 9$) of mutual Hill sphere radii $((M_{\rm i} + M_{\rm o})/3M_\star)^{1/3}(a_{\rm i} + a_{\rm o})/2$, where the subscripts i and o refer to the inner and outer planets, respectively, and ★ refers to the star (here Kepler-11). All of the observed pairs of planets satisfy this criterion, apart from the inner pair, Kepler-11b and Kepler-11c (section 4.1 of the Supplementary Information). These two planets are far enough from one another to be Hill stable in the absence of other bodies[21] (that is, in the three-body problem), and they are distant enough from the other planets that interactions between the subsystems are likely to be weak. Thus stability is possible, although by no means assured. So we integrated several systems that fit the data (given in Supplementary Table 4) for 2.5×10^8 years, as detailed in section 4.1 of the Supplementary Information. Weak chaos is evident both in the mean motions and the eccentricities (Supplementary Fig. 7), but the variations are at a low enough level to be consistent with long-term stability.

It is also of interest to determine whether this planetary system truly is as nearly coplanar as the Solar System, or perhaps even more so. Given that the planets all transit the star, they individually must have nearly edge-on orbits. As discussed above and quantified in Supplementary Table 3, the duration of planet Kepler-11e's transit implies an inclination to the plane of the sky of 88.8°, those of the two innermost planets suggest comparable inclinations, whereas those of the three other planets indicate values closer to 90°. But even though each of the planetary orbits is viewed nearly edge-on, they could be rotated around the line of sight and mutually inclined to each other. The more mutually inclined a given pair of planets is, the smaller the probability that multiple planets transit[22,23]. We therefore ran Monte Carlo simulations to assess the probability of a randomly positioned observer viewing transits of all five inner planets assuming that relative planetary inclinations were drawn from a Rayleigh distribution about a randomly selected plane. The results, displayed in Fig. 4 and Supplementary Table 6, suggest a mean mutual inclination of 1–2°. Details of these calculations are provided in section 6 of the Supplementary Information.

Mutual inclinations around the line of sight give rise to inclination changes, which would manifest themselves as transit duration changes[24]. We notice no such changes. The short baseline, small signal-to-noise ratio and small planet masses render these dynamical constraints weak at the present time for all planets but Kepler-11e. The only planet in the system with an inclination differing significantly from 90° is Kepler-11e, and we find that the duration of its transits does not change by more than 2% over the time span of the light curve. If planet Kepler-11e's orbit were rotated around the line of sight by just 2° compared to all the other components of the system, then with the masses listed in Table 1 the other planets would exert sufficient torque on its orbit to violate this limit.

Planet compositions and formation

Although the Kepler-11 planetary system is extraordinary, it also tells us much about the ordinary. Measuring both the radii and masses of small planets is extremely difficult, especially for cooler worlds farther from their star that are not heated above 1,000 K. (Very high temperatures can physically alter planets, producing anomalous properties.) The planetary sizes obtained from transit depths and planetary masses from dynamical interactions together yield insight into planetary composition.

Figure 5 plots radius as a function of mass for the five newly discovered planets the masses of which have been measured. Compared to Earth, each of these planets is large for its mass. Most of the volume of each of the planets Kepler-11c to Kepler-11f is occupied by low-density material. It is often useful to think of three classes of planetary materials, from relatively high to low density: rocks/metals, 'ices' dominated by H_2O, CH_4 and NH_3, and H/He gas. All of these components could have been accumulated directly from the protoplanetary disk during planet formation. Hydrogen and steam envelopes can also be the product of chemical reactions and out-gassing of rocky planets, but only up to 6% and 20% by mass, respectively[25]. In the Kepler-11

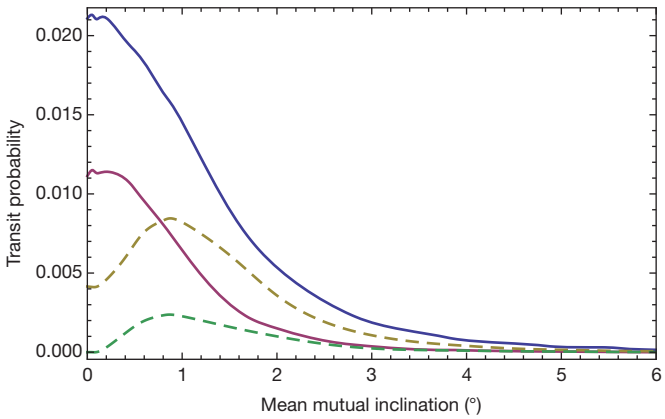

Figure 4 | Transit probabilities as a function of relative orbital inclinations of planets orbiting Kepler-11. Results of Monte Carlo simulations to assess the probability of a randomly positioned observer viewing transits of various combinations of observed and hypothesized planets around the star Kepler-11, assuming that relative planetary inclinations were drawn from a Rayleigh distribution about a randomly selected plane. The solid blue curve shows the probability of all five inner planets (Kepler-11b to Kepler-11f) to be seen transiting. The solid pink curve shows the probability of all six observed planets to be seen transiting. The ratio of the orbital period of planet Kepler-11g to that of Kepler-11f is substantially larger than that for any other neighbouring pair of transiting planets in the system. If we hypothesize that a seventh planet orbits between these objects with a period equal to the geometric mean of planets Kepler-11f and Kepler-11g, then the probability of observing transits of any combination totalling six of these seven planets is shown in the dashed golden curve. The dashed green curve shows the probability of the specific observed six planets to be seen transiting. Details of these calculations are provided in section 6 of the Supplementary Information, and numerical results are given in Supplementary Table 6.

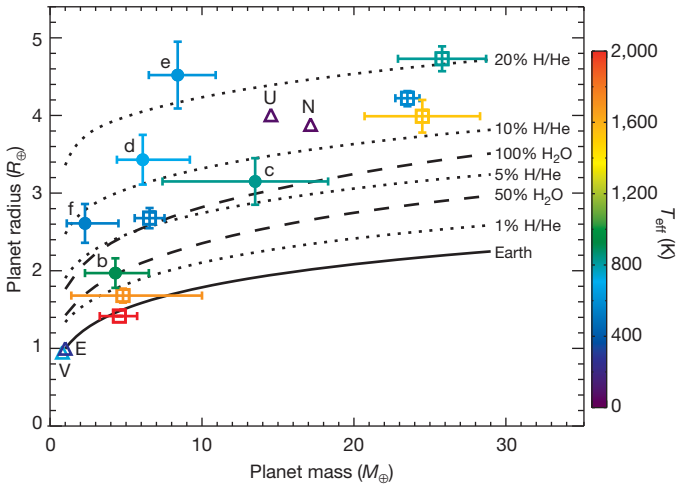

Figure 5 | Mass–radius relationship of small transiting planets, with Solar System planets shown for comparison. Planets Kepler-11b to Kepler-11f are represented by filled circles with 1σ error bars, with their letters written above; values and ranges are as given in Table 1. Other transiting extrasolar planets in this size range are shown as open squares, representing, in order of ascending radius, Kepler-10b, CoRoT-7b, GJ 1214b, Kepler-4b, GJ 436b and HAT-P-11b. The triangles (labelled V, E, U and N) correspond to Venus, Earth, Neptune and Uranus, respectively. The colours of the points show planetary temperatures (measured for planets in our Solar System, computed mean planet-wide equilibrium temperatures for Bond albedo = 0.2 for the extrasolar planets), with values shown on the colour scale on the right. Using previously implemented planetary structure and evolution models[32,33], we plot mass–radius curves for 8-Gyr-old planets, assuming $T_{eff} = 700$ K. The solid black curve corresponds to models of planets with Earth-like rock-iron composition. The higher dashed curve corresponds to 100% H_2O, using the SESAME 7154 H_2O equation of state. All other curves use a water or H_2/He envelope on top of the rock-iron core. The lower dashed curve is 50% H_2O by mass, while the dotted curves are H_2/He envelopes that make up 2%, 6%, 10% and 20% of the total mass. There is significant degeneracy in composition constrained only by mass and radius measurements[34]. Planets Kepler-11d, Kepler-11e and Kepler-11f appear to require a H_2/He envelope, much like Uranus and Neptune, while Kepler-11b and Kepler-11c may have H_2O and/or H_2/He envelopes. We note that multi-component and mixed compositions (not shown above), including rock/iron, H_2O, and H_2/He, are expected and lead to even greater degeneracy in determining composition from mass and radius alone.

system, the largest planets with measured masses, Kepler-11d and Kepler-11e, must contain large volumes of H, and low-mass planet Kepler-11f probably does as well. Planets Kepler-11b and Kepler-11c could be rich in 'ices' (probably in the fluid state, as in Uranus and Neptune) and/or a H/He mixture. (The error bars on mass and radius for Kepler-11b allow for the possibility of an iron-depleted nearly pure silicate composition, but we view this as highly unlikely on cosmogonic grounds.) In terms of mass, all five of these planets must be primarily composed of elements heavier than helium. Future atmospheric characterization to distinguish between H-dominated or steam atmospheres would tell us more about the planets' bulk composition and atmospheric stability[26].

Planets Kepler-11b and Kepler-11c have the largest bulk densities and would need the smallest mass fraction of hydrogen to fit their radii. Using an energy-limited escape model[27], we estimate a hydrogen mass-loss rate of several times 10^9 g s^{-1} for each of the five inner planets, leading to the loss of ~0.1 Earth masses of hydrogen over 10 Gyr. This is less than a factor of ten below total atmosphere loss for several of the planets. The modelling of hydrogen escape for strongly irradiated exoplanets is not yet well-constrained by observations[28,29], so larger escape rates are possible. This suggests the scenario that planets Kepler-11b and Kepler-11c had larger H-dominated atmospheres in the past and lost these atmospheres during an earlier era when the planets had larger radii, lower bulk density, and a more active primary star, which would all favour higher mass-loss rates. The comparative planetary science permitted by the planets in Kepler-11 system may allow for advances in understanding these mass-loss processes.

The inner five observed planets of the Kepler-11 planetary system are quite densely packed dynamically, in that significantly closer orbits would not be stable for the billions of years that the star has resided on the main sequence. The eccentricities of these planets are small, and the inclinations very small. The planets are not locked into low-order mean motion resonances.

Kepler-11 is a remarkable planetary system whose architecture and dynamics provide clues to its formation. The significant light-gas component of planets Kepler-11d, Kepler-11e and Kepler-11f imply that at least these three bodies formed before the gaseous component of their protoplanetary disk dispersed, probably taking no longer than a few million years to grow to near their present masses. The small eccentricities and inclinations of all five inner planets imply dissipation during the late stages of the formation/migration process, which means that gas and/or numerous bodies much less massive than the current planets were present. The lack of strong orbital resonances argues against slow, convergent migration of the planets, which would lead to trapping in such configurations, although dissipative forces could have moved the inner pair of planets out from the nearby 5:4 resonance[30]. *In situ* formation would require a massive protoplanetary disk of solids near the star and/or trapping of small solid bodies whose orbits were decaying towards the star as a result of gas drag; it would also require accretion of significant amounts of gas by hot small rocky cores, which has not been demonstrated. (The temperature this close to the growing star would have been too high for ices to have condensed.) The Kepler spacecraft is scheduled to continue to return data on the Kepler-11 planetary system for the remainder of its mission, and the longer temporal baseline afforded by these data will allow for more accurate measurements of the planets and their interactions.

Received 13 December; accepted 20 December 2010.

1. Borucki, W. J. *et al.* Kepler planet-detection mission: introduction and first results. *Science* **327,** 977–980 (2010).
2. Koch, D. G. *et al.* Kepler mission design, realized photometric performance, and early science. *Astrophys. J.* **713,** L79–L86 (2010).
3. Jenkins, J. *et al.* Overview of the Kepler science processing pipeline. *Astrophys. J.* **713,** L87–L91 (2010).
4. Caldwell, D. *et al.* Instrument performance in Kepler's first months. *Astrophys. J.* **713,** L92–L96 (2010).
5. Holman, M. J. *et al.* Kepler-9: a system of multiple planets transiting a sun-like, confirmed by timing variations. *Science* **330,** 51–54 (2010).
6. Torres, G. *et al.* Modeling Kepler transit light curves as false positives: rejection of blend scenarios for Kepler-9, and validation of Kepler-9d, a super-Earth-size planet in a multiple system. *Astrophys. J.* **727,** 24 (2011).
7. Batalha, N. *et al.* Kepler's first rocky planet: Kepler-10b. *Astrophys. J.* **728,** (in the press).
8. Steffen, J. H. *et al.* Five Kepler target stars that show multiple transiting exoplanet candidates. *Astrophys. J.* **725,** 1226–1241 (2010).
9. Mandel, K. & Agol, E. Analytic light curves for planetary transit searches. *Astrophys. J.* **580,** L171–L175 (2002).
10. Brown, T. Expected detection and false alarm rates for transiting Jovian planets. *Astrophys. J.* **593,** L125–L128 (2003).
11. Valenti, J. A. & Piskunov, N. Spectroscopy made easy: a new tool for fitting observations with synthetic spectra. *Astron. Astrophys.* **118** (Suppl.), 595–603 (1996).
12. Valenti, J. A. & Fischer, D. A. Spectroscopic properties of cool stars (SPOCS). I. 1040 F, G, and K dwarfs from Keck, Lick, and AAT planet search programs. *Astrophys. J.* **159** (Suppl.), 141–166 (2005).
13. Girardi, L., Bressan, A., Bertelli, G. & Chiosi, C. Evolutionary tracks and isochrones for low- and intermediate-mass stars: from 0.15 to 7 M_{sun}, and from Z=0.0004 to 0.03. *Astron. Astrophys.* **141** (Suppl.), 371–383 (2000).
14. Yi, S. *et al.* Toward better age estimates for stellar populations: The Y^2 isochrones for solar mixture. *Astrophys. J.* **136** (Suppl.), 417–437 (2001).
15. Holman, M. J. & Murray, N. W. The use of transit timing to detect terrestrial-mass extrasolar planets. *Science* **307,** 1288–1291 (2005).
16. Agol, E., Steffen, J., Sari, R. & Clarkson, W. On detecting terrestrial planets with timing of giant planet transits. *Mon. Not. R. Astron. Soc.* **359,** 567–579 (2005).
17. Fabrycky, D. in *Exoplanets* (ed. Seager, S.) 217–238 (University of Arizona Press, 2010).
18. Cumming, A. *et al.* The Keck planet search: detectability and the minimum mass and orbital period distribution of extrasolar planets. *Publ. Astron. Soc. Pacif.* **120,** 531–554 (2008).

19. Howard, A. *et al.* The occurrence and mass distribution of close-in super-Earths, Neptunes, and Jupiters. *Science* **330,** 653–655 (2010).
20. Smith, A. W. & Lissauer, J. J. Orbital stability of systems of closely-spaced planets. *Icarus* **201,** 381–394 (2009).
21. Gladman, B. Dynamics of systems of two close planets. *Icarus* **106,** 247–263 (1993).
22. Koch, D. & Borucki, W. A search for earth-sized planets in habitable zones using photometry. *First Int. Conf. Circumstellar Habitable Zones* 229 (Travis House Publishing, 1996).
23. Ragozzine, D. & Holman, M. J. The value of systems with multiple transiting planets. *Astrophys. J.* (submitted); preprint at ⟨http://arxiv.org/abs/1006.3727⟩ (2010).
24. Miralda-Escude, J. Orbital perturbations of transiting planets: a possible method to measure stellar quadrupoles and to detect earth-mass planets. *Astrophys. J.* **564,** 1019–1023 (2002).
25. Elkins-Tanton, L. T. & Seager, S. Ranges of atmospheric mass and composition of super-Earth exoplanets. *Astrophys. J.* **685,** 1237–1246 (2008).
26. Miller-Ricci, E., Seager, S. & Sasselov, D. The atmospheric signatures of super-Earths: how to distinguish between hydrogen-rich and hydrogen-poor atmospheres. *Astrophys. J.* **690,** 1056–1067 (2009).
27. Lecavelier des Etangs, A. A diagram to determine the evaporation status of extrasolar planets. *Astron. Astrophys.* **461,** 1185–1193 (2007).
28. Vidal-Madjar, A. *et al.* An extended upper atmosphere around the extrasolar planet HD209458b. *Nature* **422,** 143–146 (2003).
29. Lecavelier des Etangs, A. *et al.* Evaporation of the planet HD 189733 observed in H I Lyman-α. *Astron. Astrophys.* **514,** A72 (2010).
30. Papaloizou, J. C. B. & Terquem, C. On the dynamics of multiple systems of hot super-Earths and Neptunes: tidal circularization, resonance and the HD 40307 system. *Mon. Not. R. Astron. Soc.* **405,** 573–592 (2010).
31. Rowe, J. F. *et al.* Kepler observations of transiting hot compact objects. *Astrophys. J.* **713,** L150–L154 (2010).
32. Miller, N., Fortney, J. J. & Jackson, B. Inflating and deflating hot Jupiters: coupled tidal and thermal evolution of known transiting planets. *Astrophys. J.* **702,** 1413–1427 (2009).
33. Nettelmann, N., Fortney, J. J., Kramm, U. & Redmer, R. Thermal evolution and structure models of the transiting super-Earth GJ 1214b. *Astrophys. J.* (in the press); preprint at ⟨http://arxiv.org/abs/1010.0277⟩ (2010).
34. Rogers, L. A. & Seager, S. A framework for quantifying the degeneracies of exoplanet interior compositions. *Astrophys. J.* **712,** 974–991 (2010).
35. Borucki, W. J. *et al.* Characterization of planetary candidates observed by Kepler. *Astrophys. J.* (submitted).

Supplementary Information is linked to the online version of the paper at www.nature.com/nature.

Acknowledgements Kepler was competitively selected as the tenth Discovery mission. Funding for this mission is provided by NASA's Science Mission Directorate. We thank the many people who gave so generously of their time to make the Kepler mission a success. A. Dobrovolskis, T. J. Lee and D. Queloz provided constructive comments on the manuscript. D.C.F. and J.A.C. acknowledge NASA support through Hubble Fellowship grants HF-51272.01-A and HF-51267.01-A, respectively, awarded by STScI, operated by AURA under contract NAS 5-26555.

Author Contributions J.J.L. led the research effort to confirm and validate candidates as planets, assisted in the dynamical study, developed most of the interpretation and wrote much of the manuscript. D.C.F. performed dynamical analysis on transit times and derived planetary masses, derived dynamical constraints on mutual inclinations, performed long-term stability calculations, and wrote much of the Supplementary Information. E.B.F. measured transit times, including special processing for Q6 data, checked for transit duration variations, contributed to the interpretation, and supervised transit probability and relative inclination analysis. The following seven authors contributed equally: W.J.B. developed photometers, observational techniques, and analysis techniques that proved Kepler could succeed, participated in the design, development, testing and commissioning of the Kepler mission and in the evaluation of the candidates that led to the discovery of this system. F.F. modelled Kepler transit light curves as false positives leading to the rejection of blend scenarios for hierarchical triple and background configurations. G.W.M. obtained and reduced spectra that yielded the properties of the star. J.A.O. measured planet radii and impact parameters. J.F.R. performed transit searches to identify candidates, multi-candidate light curve modelling to determine stellar and planetary parameters, and transit timing measurements. G.T. modelled Kepler transit light curves as false positives, leading to the rejection of blend scenarios for hierarchical triple and background configurations. W.F.W. measured transit times and O-C curves and used Monte Carlo simulations to determine robust uncertainties. The remaining authors listed below contributed equally: N.M.B. directed target selection, KOI inspection, tracking, and vetting. S.T.B. supported centroid and light curve analysis and participated in validation discussions. L.A.B. took and analysed the first reconnaissance spectrum of the target star. D.A.C. worked on the definition and development of the Science Operations Center analysis pipeline. J.A.C. assisted in the determination of transit times and durations from the Kepler photometry. D.C. provided advice on blender analysis. J.L.C. supported the science operations to collect the Kepler data. W.D.C. obtained, reduced and analysed reconnaissance spectroscopy. J.-M.D. participated in blend studies. E.W.D. provided optical, electronic and systems support for flight segments, commissioning work, and discussions regarding validation of small planets. M.N.F. reviewed light curves and centroid time series and participated in verification and validation of the science pipeline. J.J.F. modelled the interior structure and mass-radius relationships of the planets and wrote the text on interpreting planetary structure. T.N.G. performed follow-up observation support and commissioning work. J.C.G. worked on the design of the Kepler focal plane and associated charge-coupled device (CCD) imagers and electronics. R.L.G. performed difference-image-based centroid analysis as means of discriminating against background eclipsing binary stars. M.R.H. led the team responsible for the scientific commissioning and operation of the instrument, and processing the data to produce light curves. J.R.H. developed operations procedures and processed Kepler data to produce light curves. M.J.H. developed the trending algorithm and helped in assembling and writing up the results. D.G.K. designed and developed major portions of the Kepler mission. D.W.L. led reconnaissance spectroscopy, stellar classification and the preparation of the Kepler Input Catalog. E.L. modelled the interior structure and mass–radius relations of the planets. S.McC. wrote software to manage and archive pixel and flux time series data. N.M. modelled the interior structure and mass–radius relations of the planets. R.C.M. performed transit probability versus relative inclination analysis. E.V.Q. wrote software to calibrate the pixel data to generate the flux time series. D.R. conducted data analysis and interpretation. D.S. performed calculations using stellar evolution models to determine stellar parameters. D.R.S. developed and used code to measure transit times. J.H.S. worked on validation of analysis methods and composition of text.

Author Information Reprints and permissions information is available at www.nature.com/reprints. The authors declare no competing financial interests. Readers are welcome to comment on the online version of this article at www.nature.com/nature. Correspondence and requests for materials should be addressed to J.J.L. (jack.lissauer@nasa.gov) or D.C.F. (fabrycky@ucolick.org).